A LOCAL MAXIMUM INTENSITY PROJECTION TRACING OF VASCULATURE IN KNIFE-EDGE SCANNING MICROSCOPE VOLUME DATA

Donghyeop Han, John Keyser, and Yoonsuck Choe

Texas A&M University
Department of Computer Science
College Station, TX 77843, USA

ABSTRACT

A local maximum intensity projection (MIP) approach to the extraction of a 3D vascular network, acquired by the Knife-Edge Scanning Microscope (KESM), is presented. We build a local volume for local MIP processing at each tracing step in order to reduce the dimension of input data from 3D to 2D, which leads to a 65.22% reduction of computation time compared to 3D tracing method. The proposed method makes use of existing 2D tracing methods, extending them into a 3D tracing method. Our experimental results show that our approach can rapidly and accurately extract the medial axis of vascular data acquired by the KESM.

Index Terms— Tracing, Local MIP, Dimension Reduction, Vasculature, Hessian Filter

1. INTRODUCTION

Neurovascular models have played an important role in understanding neuronal or medical conditions. Many tracing algorithms have been developed to extract the neurovascular network from 2D images. Most of them have been extended to 3D tracing methods. Frangi et al. proposed 2D and 3D tracing algorithms using a Hessian filter after convolving the input data with a Gaussian kernel [1]. Due to the second order partial derivatives in the Hessian matrix, Frangi et al.'s 3D method has a much higher computational complexity than their 2D method. Friman et al. presented multi-dimensional approach using vessel profile based on distance function [2]. In 2D, this method uses rotation matrix operations to find the vessel direction, which requires searching only a 2D plane space. However, in 3D, the rotation matrix operation requires searching a 3D spherical space, taking $O(n^2)$ processing time instead of the $O(n)$ time of the 2D method, where n is the number of sampled directions. Haris et al. presented a 2D tracing method with a circular window to extract a vascular

network [3], and Carrillo et al. extended it to 3D space using spheres [4]. In 3D, the sphere uses connected components to find the vessel direction while only a first order derivative is required on the circular window's edge in 2D. Searching the space in the sphere needs $O(r^2)$ processing time while a circular window requires $O(r)$, where r is the radius. Clearly, most 2D algorithms are more efficient than their 3D versions. In this work, we will provide a local MIP framework which makes 2D algorithm directly applicable to 3D data. Our results show that the computation time of 3D tracing can be reduced by over 60% using our proposed method.

2. METHOD

The Knife-Edge Scanning Microscope (KESM) allows the scanning of a neurovascular network of the whole mouse brain at a sub-micron resolution. An entire mouse brain ($\sim$1cm^3) can be scanned in less than 100 hours when the KESM is operating at its full capacity. Fig. 2(a) shows a full view of KESM and Fig. 2(b) shows neurovascular data of a mouse brain acquired by KESM.

The proposed method starts with automatic seed point detection and it terminates when no more seed points are detected. Each tracing iteration has the six following steps: (1) Boundary detection for obtaining local volume size, (2) Local volume evaluation, (3) Local MIP processing, (4) 2D tracing for vessel direction, (5) 3D vessel direction estimation, and (6) 3D vessel direction adjustment using a momentum operator.

Automatic seed point detection: In order to find the seed points automatically, the proposed method scans at least two slices using global thresholding for obtaining an optimal threshold to distinguish the background and the foreground objects (blood vessels). On the sampling slices, our method probes grid lines whose interval is predefined based on the maximum radius of vessel information. If a seed point detected by the threshold is already traced by another seed point, it will be ignored. Before starting the first tracing step, the seed point is adjusted by a momentum operator, which will be explained later.
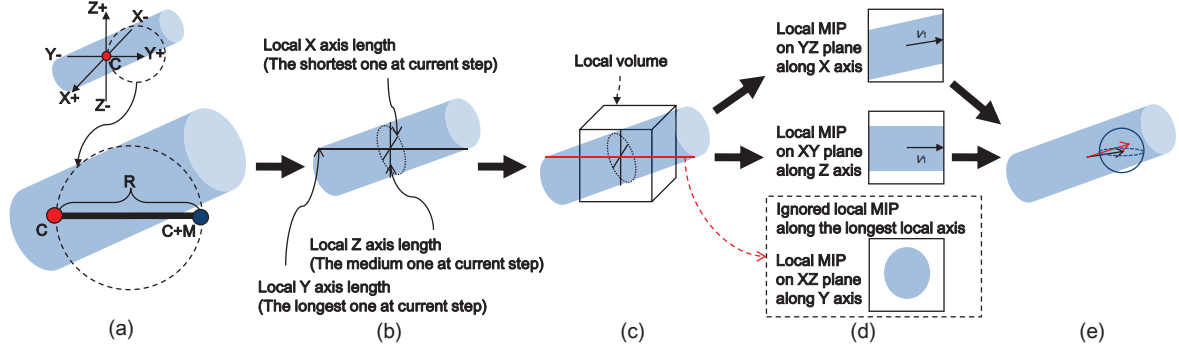
Fig. 1. Overview of each tracing step. (a) Y+ boundary detection. (b) Three local axis lengths. (c) Local volume estimation. (d) Local MIP and 2D tracing. (e) 3D vessel direction evaluation and adjustment.
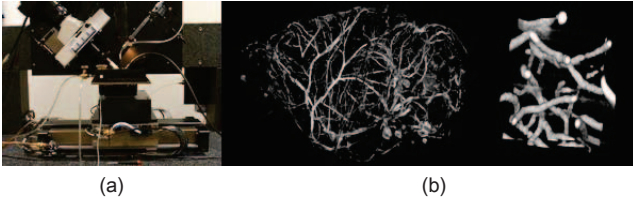

(a)   (b)

Fig. 2. (a) A full view of the Knife-Edge Scanning Microscope. (b) Saggital section of whole mouse brain vasculature (left) and a close-up of a small part of it (right).

Boundary detection and local axis length determination: At each detected seed point or center point of each tracing step, three local axis lengths can be determined along the X, Y, and Z axes (Fig. 1(b)). As described next, the distance from the Y- boundary to the Y+ boundary will be set as the local Y axis length. The local X and Z axis lengths can be obtained in a similar way. The boundary detection along each axis is key to getting the local volume correct. Moreover, the detection should be correct on both high and low contrast data. Fig. 1(a) shows how to get a Y+ boundary voxel from the center voxel C of the current tracing step using the three following probabilities. Let R denote one voxel from C (the red dot in Fig. 1(a)) to $C+M$ (the blue dot in Fig. 1(a)) along the Y+ axis. M denotes the maximum vessel radius. $C+M$ is located M voxels from C along the Y+ axis. $I_g(x)$ denotes the image intensity value at x after convolving the data with a Gaussian kernel at one-third scale of the maximum vessel radius.

$$P_{\text{in}}(C,R) = \exp\left(-\frac{(I_g(R)-I_g(C))^2}{2c^2}\right)$$
$$P_{\text{out}}(C,R) = 1 - \exp\left(-\frac{(I_g(R)-I_g(C))^2}{2c^2}\right)$$
$$P_{\text{edge}}(R,\tau)$$
$$= (1 - \exp\left(-\frac{(I_g(R+\tau)-I_g(R-\tau))^2}{2c^2}\right))/\tau \tag{1}$$

where $P_{\text{in}}(C,R)$ denotes the probability that the R voxel is inside a vessel, $P_{\text{out}}(C,R)$ denotes the probability that the R voxel is outside a vessel, and $P_{\text{edge}}(R,\tau)$ is the probability that the $(R-\tau)$ voxel is inside a vessel and $(R+\tau)$ voxel is outside a vessel. c is a constant that approximates the variance

of image intensity, which is obtained by scanning at least two slices of volumes and τ is an integer variable ($1 \leq \tau \leq M/2$). Using these probabilities, we can get the following Edge map $E(C,R)$.

$$E(C,R,\tau) = \frac{(P_{\text{in}}(C,R-\tau)+P_{\text{out}}(C,R+\tau)+P_{\text{edge}}(R,\tau))}{3}$$
$$E(C,R) = \max E(C,R,\tau),\ 1 \leq \tau \leq M/2. \tag{2}$$

So, the Y+ boundary voxel $RB(C)$ is obtained by

$$RB(C) = \operatorname*{argmax}_{R \in [C,..,C+M]} E(C,R) \tag{3}$$

If $\max E(C,R)$ is close to 0, it means that all checked points are within vessels. In that case, $RB(C)$ is set to $C+M$. The other boundary voxels are obtained in similar ways. Therefore, the local Y axis length on a voxel C is the length from the Y- boundary voxel of C to the Y+ boundary voxel of C. Fig. 3 shows how $E(C,R)$ obtains a boundary on low and high contrast images.

Local volume estimation and local MIP processing: After obtaining three local axis lengths (Fig. 1(b)) from the boundary detection, a local volume centered at voxel C is generated (Fig. 1(c)). We set (medium axis length+ζ)^3 to be the local volume size. ζ is set to 6 voxels in order for a local volume to contain background. If we set the local volume size based on either the shortest or longest axis length, local MIPs may have either no background or many vessels on each plane, making tracing difficult. In Fig. 1(c), local Z axis length is the medium axis length. Along each axis, three local MIPs can be generated on each plane (Fig. 1(d)). As seen in the dashed box in Fig. 1(d), the local MIP along the longest
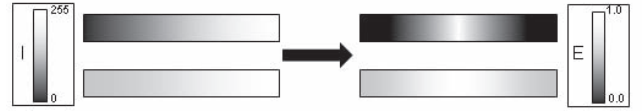

Fig. 3. Boundary detection on high and low contrast data. First row: high contrast case. Second row: low contrast case. Left column: intensity map. Right column: E(C,R) map. In the E(C,R) map, the whitest vertical line is the detected boundary.

1260

axis length (the red line in Fig. 1(c)) has little information about vessel direction. Therefore, only two local MIPs are used for selecting vessel direction.

2D tracing for vessel direction: A multiscale filter using the Hessian matrix is used for vessel direction. Let $H_\sigma(x)$ denote the Hessian matrix at a voxel x with scale σ:

$$H_\sigma = \begin{bmatrix} I_{xx} & I_{xy} \\ I_{yx} & I_{yy} \end{bmatrix}, I_{\alpha\beta}(x) = \sigma^2 \frac{\delta^2 G(x,\sigma)}{\delta\alpha\delta\beta} I(x) \quad (4)$$

where $G(x,\sigma)$ is the Gaussian kernel based on scale-space theory. The eigenvector v_1 corresponding to the smallest magnitude eigenvalue λ_1, and it indicates the vessel direction. Frangi et al. presented vessel likeliness function $V(x,\sigma)$ using geometric ratios R_B [1]:

$$V(x,\sigma) = \begin{cases} 0 & \text{if } \lambda_2 > 0, \\ \exp\left(-\frac{R_B^2}{2\beta^2}\right)\left(1 - \exp\left(-\frac{S^2}{2c^2}\right)\right) \end{cases}$$

(5)

where $R_B = \lambda_1/\lambda_2$ is the blobness measure in 2D and $S = \sqrt{\sum_{i=1}^{2} \lambda_i^2}$ is the second order structure measurement. β and c control the sensitivity of the Hessian filter and we set them to 0.5 and 0.25 respectively. The maximum value among $V(x,\sigma)$ at scale σ gives the eigenvector v_1 which is the vessel direction.

3D vessel direction estimation and adjustment: Let us take an example in which the local MIPs on XY and YZ plane are used (Fig. 1(d)). As stated above, in this example, the local MIP on XZ plane is ignored because it has little information about vessel direction (the dashed box in Fig. 1(d)). Let V_{xy} and V_{yz} be the eigenvectors of the Hessian matrix on XY and YZ plane respectively. V_{xy} and V_{yz} have $(x_1, y_1, 0)$ and $(0, y_2, z_2)$ unit vectors after normalization. The 3D vessel direction V_{xyz} is derived as $V_{xyz} = (x_1, (y_1 + y_2)/2, z_2)$. Therefore, the ith center point C^i is evaluated as

$$C^i = \frac{V_{xyz}}{\|V_{xyz}\|}\rho + C^{i-1} \quad (6)$$

where step size ρ is set to 3 voxels (black arrow in Fig. 1(e)). Due to the discretization error of MIP, we use a momentum operator to adjust the center point within a spherical window (red arrow in Fig. 1(e)) [5]. The adjusted local center $(\bar{x}, \bar{y}, \bar{z})$ is given by

$$(\bar{x}, \bar{y}, \bar{z}) = (\frac{M_{100}}{M_{000}}, \frac{M_{010}}{M_{000}}, \frac{M_{001}}{M_{000}}) \quad (7)$$

where M_{pqr} is derived as

$$M_{pqr} = \int_z \int_y \int_x x^p y^q z^r f(x,y,z) dxdydz. \quad (8)$$

We consider $f(x,y,z)$ as an intensity value at the (x,y,z) location.

Stopping criteria: When the maximum response among $V(x,\sigma)$ is less than a predefined threshold or the current step
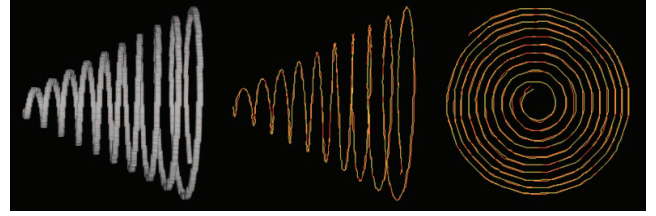

Fig. 4. Local MIP traces. Left: Synthetic data. Middle: Trace result. The red one is the trace result of a 2D version of Frangi et al.'s method with our local MIP processing. The yellow one is the trace result of a 3D version of Frangi et al.'s method. Right: The same trace result seen from a different view.

Fig. 5. Trace comparison. Left: Mouse cerebellum data obtained by KESM. Volume size is 128^3 voxels. Voxel size is $0.6\mu m \times 0.7\mu m \times 1.0\mu m$. Middle: The trace result of a 3D version of Frangi et al.'s method. Right: The trace result of a 2D version of Frangi et al.'s method with our local MIP processing.

comes across one of the previous trace results, tracing terminates and the algorithm tries to find other seed points for new tracing. The predefined threshold is set to 0.3. Note that if other existing 2D tracing algorithms are used, their stopping criteria can be used for the proposed method.

3. RESULT

We traced examples on a PC with an Intel Pentium 4 (2.4 GHz) processor, 512MB of memory, and Windows XP operating system. The C/C++ programming language and OpenGL graphics library were used.

Synthetic data tracing result: The synthetic data size is 256^3 and has curvature range from 0.001 to 0.1 with 5 voxel width. Fig. 4 shows the result of the proposed method (Frangi et al.'s 2D tracing method with local MIP processing (red line)) and the result of Frangi et al.'s 3D tracing method (yellow line). Note that the 2D tracing result with local MIP is very similar to the 3D tracing result.

Performance comparison: The size of a mouse cerebellum vascular volume acquired by KESM is 128^3 voxels. Fig. 5 shows one volume with trace results. In this case, the proposed method took 188.05 sec for 1188 voxels while the 3D tracing method took 484.69 sec for 1065 voxels. Note that Fig. 6 shows how significantly the proposed method reduces processing time compared with a 3D method. This improvement is due to the fact that the 3D method uses a 3×3 Hessian matrix with 3D Gaussian kernel ($O(n^3)$) while the proposed
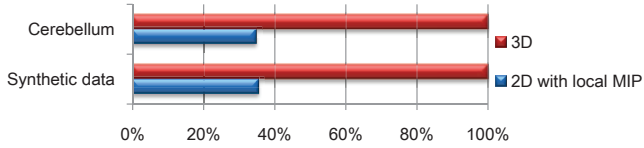
1261

Fig. 6. Performance comparison (processing time). 3D processing time is set to 100%. The proposed method takes 34.78% and 35.40% of 3D processing time for the cerebellum and the synthetic data, respectively.
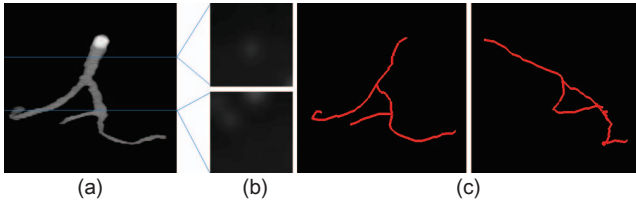

Fig. 7. Low contrast data trace. (a): 3D vascular data. (b): Two sample slices of (a). Gaussian blur (σ=30) was applied in all slices for low contrast. The first sample slice has 47.9 (μ) intensity with 4.5 (σ). The second sample slice has 49.1 (μ) intensity with 6.9 (σ). (c): Trace result with the proposed method from two views.

method uses a 2×2 Hessian matrix with 2D Gaussian kernel ($O(n^2)$), where n is the scale of Gaussian filter. Other tracing algorithms can have similar results due to dimension reduction. For example, Friman et al.'s method will have a similar performance with local MIP processing because the 3D version has $O(n^2)$ processing time while the 2D version is $O(n)$, where n is the number of sampled directions in 2D space [2]. Similarly, local MIP processing can also be used with Koller et al.'s method [6].

Low contrast data: Due to uneven illumination, KESM sometimes yields low contrast images. The boundary detection part should evaluate correct local volumes so that the proposed method can trace a 3D volume correctly. Fig. 7 shows the tracing result on a low contrast volume.

Validation: The following experiments were conducted for validating the proposed method. Two individuals manually select the centerline points for 10 pieces of vascular data. We used two measurements (length difference:ϕ and centerline deviation:φ) to quantitatively evaluate the difference between the proposed method's result (A) and two manual results (R1, R2) based on Zhang et al.'s validation [7]. The length difference (ϕ) is derived as $\phi = |1 - L_R/L_A|$, where L_R and L_A are the length of vascular data extracted by person and the proposed method respectively. The centerline deviation (φ) is defined as $\varphi = V_{ox}(L_R, L_A)/L_A$, where $V_{ox}(L_R, L_A)$ is the total number of voxels between L_R and L_A. Table 1 shows how different our method's result is from the manual results. p-values are evaluated using a two-sided paired t-test, which shows that two manual results are similar (no significant difference). Table 2 shows that there is strong correlation between the proposed method's result and the manual results.

Table 1. The mean (μ) and standard deviation (σ) length difference and centerline deviation values for two manual results (R1 & R2)

	ϕ			φ		
	μ	σ	p-value	μ	σ	p-value
R1	0.1518	0.1762	0.4188	1.2131	0.3529	0.6853
R2	0.1325	0.1804		1.1294	0.3016	

Table 2. Correlation coefficients between our method (A) and manual ground truths (R1 & R2)

	ϕ			φ		
	A	R1	R2	A	R1	R2
A	-	0.9917	0.9904	-	-	-
R1	0.9917	-	0.9982	-	-	0.9740
R2	0.9904	0.9982	-	-	0.9740	-

4. CONCLUSION

Our main contribution is the local maximum intensity projection framework we presented for tracing the vascular data in a 3D volume. The framework makes most existing 2D tracing algorithms directly applicable to 3D vascular data tracing, with better performance compared to their 3D tracing counterparts in terms of speed. The tracing is also accurate compared to the manual method, which can make the proposed method suitable for rapidly and accurately performing the extraction of 3D vascular data. In future work, we will consider situations where current 3D tracing algorithms may have better tracing results than ours, such as stenosis and branch points.

5. REFERENCES

[1] A. F. Frangi, W. J. Niessen, R. M. Hoogeveen, T. V. Walsum, and M. A. Viergever, "Model-based quantification of 3-d magnetic resonance angiographic images," *IEEE Trans. Med. Imag.*, vol. 18, pp. 946–956, 1999.

[2] O. Friman, M. Hindennach, and H. O. Peitgen, "Template-based multiple hypotheses tracking of small vessels," *IEEE ISBI*, pp. 1047–1050, May 2008.

[3] K. Haris, S. N. Efstratiadis, N. Maglaveras, C. Pappas, J. Gourassas, and G. Louridas, "Model-based morphological segmentation and labeling of coronary angiograms," *IEEE Trans. Med. Imag.*, vol. 18, pp. 1003–1015, October 1999.

[4] J. F. Carrillo, M. H. Hoyos, E. E. Davila, and M. Orkisz, "Recursive tracking of vascular tree axes in 3d medical images," *IJCARS*, pp. 331–339, 2007.

[5] C. Boldak, Y. Rolland, and C. Toumoulin, "An improved model-based vessel tracking algorithm with application to computed tomography angiography," *JBBE*, pp. 41–64, 2003.

[6] T. M. Koller, G. Gerig, G. Szekely, and D. Dettwiler, "Multiscale detection of curvilinear structures in 2-d and 3-d image-data," *ICCV*, pp. 864–869, 1995.

[7] Y. Zhang, X. Zhou, J. Lu, J. Lichtman, D. Adjeroh, and S. Wong, "3-d axon structure extraction and analysis in confocal fluorescence microscopy images," *LSSA Workshop*, pp. 241–244, 2007.